

1. Report No. FHWA/TX-03/4904-2		2. Government Accession No.		3. Recipient's Catalog No.	
4. Title and Subtitle CORROSION PERFORMANCE OF POLYMER-COATED, METAL-CLAD AND OTHER REBARS AS REINFORCEMENT IN CONCRETE				5. Report Date May 2000	
				6. Performing Organization Code	
7. Author(s) P. G. Deshpande, J. D. Seddelmeyer, H. G. Wheat, D. W. Fowler, and J. O. Jirsa				8. Performing Organization Report No. Research Report 4904-2	
9. Performing Organization Name and Address Center for Transportation Research The University of Texas at Austin 3208 Red River, Suite 200 Austin, TX 78705-2650				10. Work Unit No. (TRAIS)	
				11. Contract or Grant No. Research Project 7-4904	
12. Sponsoring Agency Name and Address Texas Department of Transportation Research and Technology Implementation Office P.O. Box 5080 Austin, TX 78763-5080				13. Type of Report and Period Covered Research Report (3/99-8/99)	
				14. Sponsoring Agency Code	
15. Supplementary Notes Project conducted in cooperation with the U.S. Department of Transportation, the Federal Highway Administration, and the Texas Department of Transportation.					
16. Abstract Corrosion of reinforcement in concrete has been a matter of great concern in recent years owing to the increase in consumption of deicing salts on highways and bridges in the United States. The problem has been traced to corrosion of reinforcement caused by chlorides present in deicing salts. Various polymer coatings and metal claddings have been proposed (by independent suppliers) in this project with a view to minimize the damage caused to reinforcements in concrete from corrosion owing to chlorides. Coatings include zinc (galvanized), several epoxies, polyvinyl chloride (PVC) coating, and Nylon 11 coating. A stainless steel-clad material is also included as well as pure stainless steel reinforcement bar. The corrosion performance tests include extensive macrocell testing, immersion tests of the polymer-coated rebars, and polarization resistance tests for the metallic rebars.					
17. Key Words Corrosion, steel, concrete, alternative materials			18. Distribution Statement No restrictions. This document is available to the public through the National Technical Information Service, Springfield, Virginia 22161.		
19. Security Classif. (of report) Unclassified		20. Security Classif. (of this page) Unclassified		21. No. of pages 68	22. Price

**CORROSION PERFORMANCE OF POLYMER-COATED,
METAL-CLAD AND OTHER REBARS AS
REINFORCEMENTS IN CONCRETE**

by

P. G. Deshpande

J. D. Seddelmeyer

H. G. Wheat

D. W. Fowler

J. O. Jirsa

Research Report 4904-2

Research Project 7-4904

“Feasibility of Hot Dipped (Zinc) Galvanizing and Other Coatings for the Protection of
Reinforcing Steel”

Conducted for the
Texas Department of Transportation
in cooperation with
U.S. Department of Transportation
Federal Highway Administration
by the
Center for Transportation Research
Bureau of Engineering Research
The University of Texas at Austin

May 2000

DISCLAIMERS

The contents of this report reflect the views of the authors, who are responsible for the facts and the accuracy of the data presented herein. The contents do not necessarily reflect the official views or policies of the Federal Highway Administration or the Texas Department of Transportation (TxDOT). This report does not constitute a standard, specification, or regulation.

There was no invention or discovery conceived or first actually reduced to practice in the course of or under this contract, including any art, method, process, machine, manufacture, design or composition of matter, or any new and useful improvement thereof, or any variety of plant, which is or may be patentable under the patent laws of the United States of America or any foreign country.

NOT INTENDED FOR CONSTRUCTION, BIDDING, OR PERMIT PURPOSES

Harovel Wheat, P.E (Texas No. 78364)

James O. Jirsa, P.E (Texas No. 31360)

David Fowler, P.E (Texas No. 27859)

Research Supervisors

ACKNOWLEDGMENTS

The researchers are grateful for the support of TxDOT and the efforts of Robert Sarcinella and Lloyd Wolf.

Prepared in cooperation with the Texas Department of Transportation and the U.S. Department of Transportation, Federal Highway Administration.

TABLE OF CONTENTS

1. Chapter 1: INTRODUCTION.....	1
1.1 INTRODUCTION.....	1
1.2 RESEARCH OBJECTIVES.....	2
1.3 CORROSION OF REINFORCING STEEL IN CONCRETE.....	3
2. Chapter 2: MACROCELL CORROSION STUDY: PRINCIPLE, TEST RESULTS AND DISCUSSION.....	5
2.1 INTRODUCTION.....	5
2.2 SCOPE.....	6
2.2.1 Corrosion Resistant Materials.....	6
2.2.2 Bar Configurations.....	7
2.2.3 Bar Size.....	9
2.3 DESIGN OF MACROCELL SPECIMENS.....	16
2.4 CONSTRUCTION OF MACROCELL SPECIMENS.....	18
2.4.1 Bar Preparation.....	18
2.4.2 Formwork and Bar Placement.....	21
2.4.3 Concrete Casting.....	24
2.4.4 Saltwater Reservoir.....	27
2.4.5 Electrical Wiring.....	27
2.4.6 Storage.....	28
2.5 MATERIAL PROPERTIES.....	29
2.5.1 Bar Properties.....	29
2.5.2 Concrete Properties.....	33
2.6 EXPERIMENTAL PROGRAM.....	35
2.6.1 Chloride Exposure.....	35
2.6.2 Corrosion Monitoring.....	38
2.6.3 Additional Testing.....	39

2.7 TEST RESULTS.....	40
3. Chapter 3: CORROSION EVALUATION USING POLARIZATION RESISTANCE: PRINCIPLE, TEST RESULTS AND DISCUSSIONS.....	42
3.1 INTRODUCTION.....	42
3.1.1 History and Description.....	42
3.1.2 Test Set-Up.....	43
3.1.3 Electrolyte / Solution.....	44
3.2 TEST PROCEDURE.....	45
3.3 TEST RESULTS.....	50
3.3.1 Black Rebar.....	50
3.3.2 Pure Stainless Steel 304 Rebar.....	52
3.3.3 Galvanized “A” Coated Rebar.....	55
3.3.4 Galvanized “B” Coated Rebar.....	57
3.3.5 Comparison of all Systems.....	59
4. Chapter 4: SUMMARY AND CONCLUSIONS.....	62
4.1 SUMMARY OF EXPERIMENTAL RESULTS.....	62
4.1.1 Summary of Macrocell Testing.....	62
4.1.2 Summary of Polarization Resistance and Screening Tests.....	62
REFERENCES.....	64

LIST OF FIGURES

Figure 1.1:	The Energy Cycle of Iron indicating It Is Extractive Metallurgy in Reverse.....	3
Figure 2.1:	Black Steel Reinforcement Bar.....	11
Figure 2.2:	Epoxy-Coated Reinforcement Bar A.....	11
Figure 2.3:	Epoxy-Coated Reinforcement Bar B.....	12
Figure 2.4:	Nonbendable Epoxy-Coated Reinforcement Bar.....	12
Figure 2.5:	Nylon 11 Coated Reinforcement Bar.....	13
Figure 2.6:	PVC-Coated Reinforcement Bar.....	13
Figure 2.7:	Galvanized-Coated Reinforcement Bar A.....	14
Figure 2.8:	Galvanized-Coated Reinforcement Bar B.....	14
Figure 2.9:	Galvanized-Coated Reinforcement Bar B.....	15
Figure 2.10:	Galvanized-Coated Reinforcement Bar B.....	15
Figure 2.11:	Typical Project 1265 Macrocell Specimen.....	17
Figure 2.12:	Separation of Stainless Steel Cladding from Shearing.....	20
Figure 2.13:	Typical Formwork for Macrocells with #4 Bars.....	22
Figure 2.14:	Typical Formwork for Macrocells with #6 Bars.....	23
Figure 2.15:	Macrocell Concrete Placement.....	25
Figure 2.16:	Curing of Macrocell Specimen.....	26
Figure 2.17:	Completed Macrocell Specimen.....	28
Figure 2.18:	Macrocell Storage Racks.....	29
Figure 2.19:	Digital Calipers and Coating Thickness Gage.....	31
Figure 2.20:	Researcher Making 3.5% NaCl Solution at the Beginning of the “Wetting Cycle”.....	35
Figure 2.21:	Researcher Pouring 3.5% NaCl Solution in Dikes at Beginning of “Wetting Cycle”.....	36
Figure 2.22:	Student Placing Plywood Sheet over Macrocell-Filled Dikes to Minimize Evaporation.....	36
Figure 2.23:	Macrocells with One Bent Black Rebar as Top-Reinforcing Layer and None in the Bottom-Reinforcing Layer.....	37

Figure 2.24: Macrocells with Two Straight Black Rebars as Bottom-Reinforcing Layer and None in the Top-Reinforcing Layer.....	38
Figure 2.25: Multimeter.....	39
Figure 3.1: Schematic Diagram of Polarization Resistance Test Cell.....	44
Figure 3.2: Polymer-Coated Rebars with Their Tips Polished to Ensure Good Electrical Contact during Polarization Resistance Test.....	45
Figure 3.3: Polarization Resistance Test Cells without Connections.....	46
Figure 3.4: Polarization Resistance Test Cells with Connections.....	46
Figure 3.5: Lid of Polarization Resistance Test Cell with Holes to Accommodate the Rebar, the Reference Electrode and the Lugin Probe.....	48
Figure 3.6: Corr. Rate and PR versus Salt Concentration for Black Steel.....	50
Figure 3.7: Corr. Rate versus No. of Days for Black Steel.....	52
Figure 3.8: Corr. Rate and PR versus Salt Concentration for SS304 Rebar.....	53
Figure 3.9: Corr. Rate versus No. of Days for SS304 Rebar.....	55
Figure 3.10: Corr. Rate and PR versus Salt Concentration for Galvanized A Rebar.....	56
Figure 3.11: Corr. Rate versus No. of Days for Galvanized A Rebar.....	57
Figure 3.12: Corr. Rate and PR versus Salt Concentration for Galvanized B Rebar.....	58
Figure 3.13: Corr. Rate versus No. of Days for Galvanized B Rebar.....	59
Figure 3.14: Comparison of Corrosion Rates of Various Rebars.....	60

LIST OF TABLES

Table 2.1:	Schedule of Macrocell Test Specimens.....	10
Table 2.2:	ASTM A615 and A775 Requirements.....	30
Table 2.3:	Measured Bar Deformation and Coating Properties.....	32
Table 2.4:	Concrete Batch Data.....	33
Table 2.5:	Conditions during Macrocell Casting.....	34
Table 2.6:	Macrocell Concrete Compressive Strength.....	34
Table 2.7:	Macrocell Ponding Test.....	40
Table 3.1:	Density and Equivalent Weight of Various Materials.....	47
Table 3.2:	PR Sample Test Sheet (for Black Steel).....	49
Table 3.3:	Corrosion Rate and PR versus Salt Concentration.....	50
Table 3.4:	Corrosion Rate versus No. of Days for Black Steel.....	51
Table 3.5:	Corrosion Rate and PR versus Salt Concentration for SS304.....	53
Table 3.6:	Corrosion Rate versus No. of Days for SS304.....	54
Table 3.7:	Corrosion Rate and PR versus Salt Concentration for Galv. A Rebar.....	55
Table 3.8:	Corrosion Rate versus No. of Day for Galv. A Rebar.....	56
Table 3.9:	Corrosion Rate and PR versus Salt Concentration for Galv. B Rebar.....	57
Table 3.10:	Corrosion Rate versus No. of Days for Galv. B Rebar.....	58
Table 3.11:	Corrosion Rate versus Salt Concentration (of All Systems).....	59

Chapter 1:

Introduction

1.1 INTRODUCTION

Corrosion of reinforcement in concrete has been a matter of great concern in recent years because of the increase in the consumption of deicing salts on highways and bridges in the United States. The problem has been traced to corrosion of reinforcement caused by chlorides present in deicing salts. Despite its disastrous effect on reinforcement, salts are still used extensively to keep the roads clear of snow in harsh winters.

An alternative to the use of black steel reinforcement is the use of epoxy-coated reinforcing steel in concrete. Epoxy-coated rebar was incorporated as a corrosion protection measure for reinforcement in extremely aggressive environments, and thus epoxy-coated rebars were used by most states, including the Florida Department of Transportation (FDOT) in the construction of several bridges in Florida in 1970 (Mc Donald et al. 1995).

However, corrosion spalls began to appear in the substructure of bridges built with epoxy-coated rebars. Several investigations were commissioned by FDOT to address the causes of the unexpected development of corrosion in the Florida Keys bridges. Partly as a result of this experience, various other investigations of performance of epoxy-coated rebars were initiated (Lee and Hartt 1998).

It is evident that using epoxy-coated rebars does not always prevent corrosion in aggressive environments. Hence, a need arises to evaluate the corrosion performance of other coatings and claddings such as polyvinyl chloride (PVC)-coated rebars, nylon-coated rebars, pure stainless steel rebars, stainless steel-clad rebars, and galvanized rebars.

1.2 RESEARCH OBJECTIVES

During 1998, a research project sponsored by the Texas Department of Transportation (TxDOT), was initiated to evaluate the performance of certain reinforcement coatings and claddings provided by independent suppliers. The main objective of this project (which was carried out by The University of Texas at Austin and funded by TxDOT) was to investigate the corrosion performance of these particular materials, especially in the presence of chloride ions.

It was decided to carry out three types of tests: macrocell testing, polarization resistance (PR) testing, and pull-out testing.

- The **macrocell testing** was used to evaluate the current flow as a function of time and presumably chloride concentration. Thus, it performs almost real-time analysis of the corrosion behavior of these materials in concrete when exposed to chloride ions.
- For **immersion testing**, bars were evaluated based on their behavior in salt-free and salt-contaminated solutions, which simulate concrete (e.g., calcium hydroxide) for various times.
- In the case of the metallic materials, another type of test, **PR** was carried out. As a result of this test, the corrosion rate (which is inversely related to PR) of the metallic materials in various electrolytes or environments can be estimated.
- A rebar with a coating, which has an excellent performance against corrosion in a chloride environment, would have little use if it fails to have adequate bond with the surrounding concrete. Hence, a third type of test, the **pull-out**, was carried out in a companion study to determine the bond between the different rebar systems and concrete.

1.3 CORROSION OF REINFORCING STEEL IN CONCRETE

At present, the greatest extent of natural damage to reinforced concrete structures can be attributed to chloride ions. Transportation structures and parking garages in cold climates are damaged because of deicing salts. Coastal structures and bridge substructures in marine environments are damaged by seawater and salt spray. In addition, structures are often constructed with a built-in destructive agent: a chloride-based accelerating admixture. Moreover, self-contaminated aggregates and brackish water set the stage for advanced corrosion and premature durability problems.

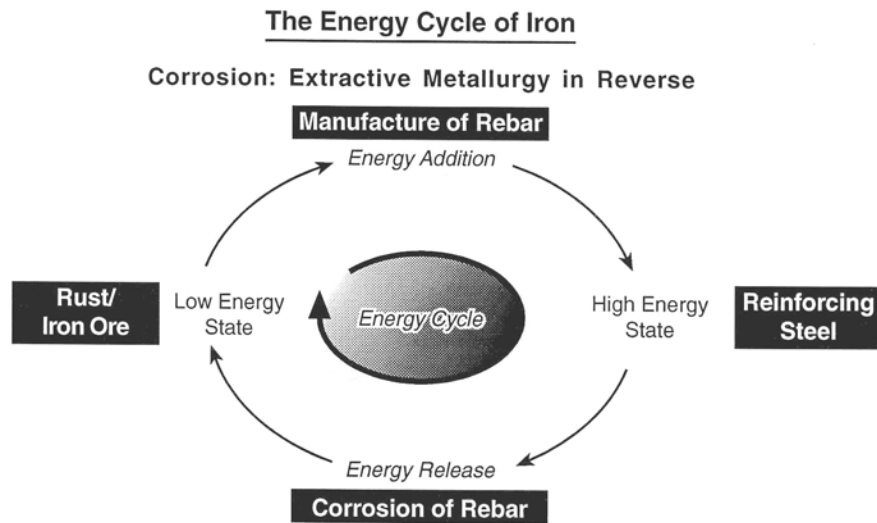


Figure 1.1: The Energy Cycle of Iron Indicating It Is Extractive Metallurgy in Reverse (Kahhaleh et al. 1994)

Corrosion of metals may be considered as extractive metallurgy in reverse (Fontana 1986). The process is described in Figure 1.1. Hence, the solution to corrosion problems may not always be in their total elimination (as this may be a difficult task). Rather, the answer may lie in a goal to find the most efficient way of living with them so as to cause minimal damage.

Chapter 2:

Macrocell Corrosion Study:

Principle, Test Result and Discussions

2.1 INTRODUCTION

Concrete and bridge structures are exposed to large amounts and varying concentrations of deicing salts in regions with snowfall. This leads to exposure of concrete and its reinforcement to chlorides. It has been known that chlorides accelerate corrosion (or the onset of corrosion) on the reinforcement surface. As a result, there is rust formation, which has a greater volume than the original steel. Hence, there is stress induced, causing cracking of concrete, in turn making it an even more open structure for the penetration of chlorides.

Therefore, it is necessary to design an experiment that will simulate optimum real-life conditions. One such experiment is the macrocell test, which is described in ASTM G109 (ASTM 1999). This test makes use of two layers of steel, one close to a chloride source and the other much farther from the chloride source. This test has become a very popular test for studying the behavior of steel in concrete.

There have been numerous research projects to study the corrosion resistance of an individual coating or metal for concrete reinforcement protection, but relatively few projects have tested numerous materials of different types to make comparisons and determine which ones offer better corrosion performance. This long-term corrosion study involves the testing of 176 macrocell specimens to compare the corrosion resistance of different metallic coatings, organic coatings, and corrosion resistant steels.

2.2 SCOPE

The objective of the macrocell test program was to compare the resistance of different coatings and metals to corrosion when embedded in concrete. The purpose was to identify which materials provide better protection for concrete-reinforcing steel.

Care was taken in the design and construction of the macrocell specimens so that each specimen was as identical as possible. The only variable being tested was the type of corrosion resistant bar. The macrocell specimens were grouped according to the type of corrosion resistant bar. Sixteen macrocells were constructed for each type of corrosion resistant bar. Within each of these groups of macrocells are different bar-coupling configurations. The control group consisted of uncoated bars with normal mill scale. Eight macrocells were constructed for each of the control groups.

2.2.1 Corrosion Resistant Materials

Early in the project, reinforcing bar coatings and metals marketed for purposes of corrosion protection were identified. Letters were sent to the manufacturers of these materials that contained information about this research project and an invitation to submit materials for testing. The manufacturers were asked to submit a minimum amount of material required to construct both the macrocell specimens and the pull-out specimens.

Three metal-coating systems were received. Two different manufacturing facilities submitted hot-dipped galvanized bars. Type 304 stainless steel-clad bars were also received.

Five organic-coating systems were received. Two of the organic coatings were fusion-bonded epoxies manufactured by two different companies. Nonbendable epoxy-coated bars were received. This type of epoxy is harder and more brittle than typical epoxy coatings. To prevent cracking in the nonbendable epoxy, bars must be bent to the desired shape prior to coating. Polyvinyl chloride (PVC) and nylon-coated bars were also received.

One type of corrosion resistant metal, type 304 stainless steel, was received and included in the study as well as a stainless steel-clad rebar.

A second corrosion resistant metal, ferritic steel, was received. However, the ferritic steel bars were received after the concrete had been cast for the macrocell specimens, and therefore were not included in this project.

2.2.2 Bar Configurations

Within each group of macrocells, except the control group, there were different configurations of electrically coupled bars. All of the macrocell specimens had corrosion resistant bars for the top layer of steel. However, different configurations of bars were used for the bottom layer of steel. The purpose was to determine if the corrosion of reinforcement was affected by different bar configurations typically found in practice and, if so, to determine which configurations experience the least corrosion.

Fifty percent of the macrocell specimens for each group of corrosion resistant bars were constructed with uncoated mild steel bars for the bottom layer of steel. These specimens were intended to simulate concrete members, such as bridge decks, that might have corrosion resistant bars for the top layer of reinforcement but uncoated mild steel bars for the bottom layer. This situation might occur because corrosion resistant bars cost more and using typical mild steel bars for the bottom layer of reinforcement results in a cost savings.

Twenty-five percent of the specimens were constructed with corrosion resistant bars for the bottom layer. These specimens were intended to simulate concrete members for which all of the reinforcement was specified to be corrosion resistant.

The remaining 25 percent of specimens were built without a bottom layer of steel. These specimens will be coupled to another macrocell that has not been exposed to chlorides or has only uncoated mild steel bars on the bottom layer. Coupling these two macrocells simulates deeper members, such as beams, that have chloride-contaminated concrete near the top surface and uncontaminated concrete at greater depths. In addition, the ability to couple different macrocells, such as epoxy and galvanized, offers much more flexibility.

Macrocell configurations for each of the corrosion resistant and control groups can be seen in Table 2.1. Photographs of various reinforcement bars used in this research project are shown in Figures 2.1 through 2.10.

2.2.3 Bar Size

The results of the macrocell study in TxDOT Project 1265 indicated that the corrosion rate is influenced by the diameter of the bar (Gowripalan 1998). Therefore, a single bar size is

needed for direct comparisons of different corrosion resistant materials. The galvanized coating, organic coatings, and solid 304 stainless steel were tested using #4 bars (1/2-inch diameter). The bar size of the uncoated mild steel bars used for the control group was also #4.

Table 2.1: Schedule of Macrocell Test Specimens

Bar Type	Bar Size	Top: Resistant Steel Bottom: Black Steel	Top: Resistant Steel Bottom: Resistant Steel	Top: Resistant Steel Bottom: No Steel	Top: No Steel Bottom: Black Steel
Control A (Black Steel)	4	4*	0	2**	2
Galvanized A	4	8	4	4	0
Galvanized B	4	8	4	4	0
Epoxy A	4	8	4	4	0
Epoxy B	4	8	4	4	0
Nonbendable Epoxy	4	8	4	4	0
Nylon	4	8	4	4	0
PVC	4	8	4	4	0
304 Stainless Steel	4	8	4	4	0
Control B (Black Steel)	6	4*	0	2**	2
Epoxy A	6	8	4	4	0
304 Stainless Steel-Clad	6	8	4	4	0

* Black steel on top and bottom

** Black steel on top



Figure 2.1: Black Steel Reinforcement Bar



Figure 2.2: Epoxy-Coated Reinforcement Bar A



Figure 2.3: Epoxy-Coated Reinforcement Bar B



Figure 2.4: Nonbendable Epoxy-Coated Reinforcement Bar

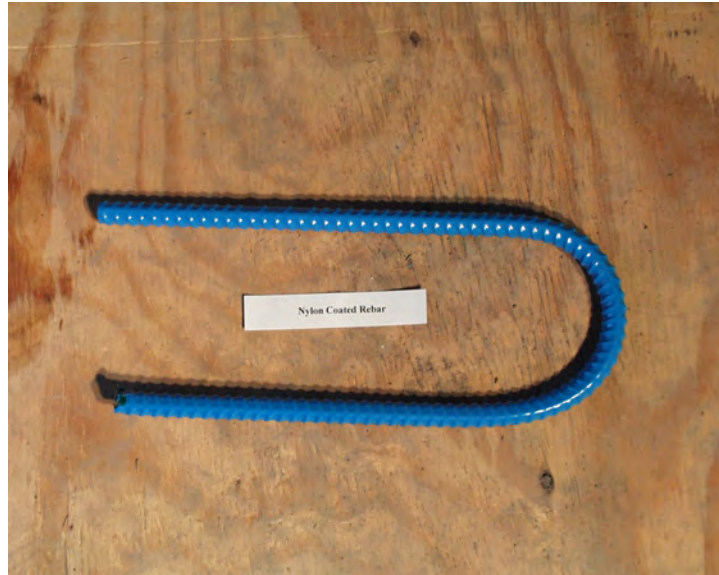


Figure 2.5: Nylon 11 Coated Reinforcement Bar



Figure 2.6: PVC-Coated Reinforcement Bar



Figure 2.7: Galvanized-Coated Reinforcement Bar A



Figure 2.8: Galvanized-Coated Reinforcement Bar B



Figure 2.9: Pure Stainless Steel 304 Reinforcement Bar



Figure 2.10: Stainless Steel 304 Clad Reinforcement Bar

The 304 stainless steel cladding was available only in a #6 bar size (3/4-inch diameter). Because of differences in the bar size, direct comparisons were not possible between the #6 stainless steel-clad bars and the #4 bars. Therefore, an additional control group and an additional epoxy-coated group were cast using #6 bars to eliminate bar size as a variable for evaluating the stainless steel-clad group.

2.3 DESIGN OF MACROCELL SPECIMENS

The design of the macrocell specimens in this project was based on the macrocell specimens tested in Project 1265, “Structural Integrity of Epoxy-Coated Bars,” at the University of Texas at Austin (Vaca-Cortes 1999). In this project, macrocell specimens were successfully used to determine the effects of damage, different bar sizes, and different bar deformations on the corrosion resistance of epoxy-coated bars.

A schematic diagram of the macrocell specimen from Project 1265 can be seen in Figure 2.11. The overall dimensions of the macrocell used in this program were 10 inches long by 9 inches wide by 8 inches high. The macrocell consisted of two layers of steel bars embedded in a concrete prism. The top layer was a single bar that had been bent into a “U” shape. Both ends of the “U”-shaped bar protruded from the concrete prism. The bottom layer consisted of two straight bars. One end of each bottom straight bar protruded from the concrete prism.

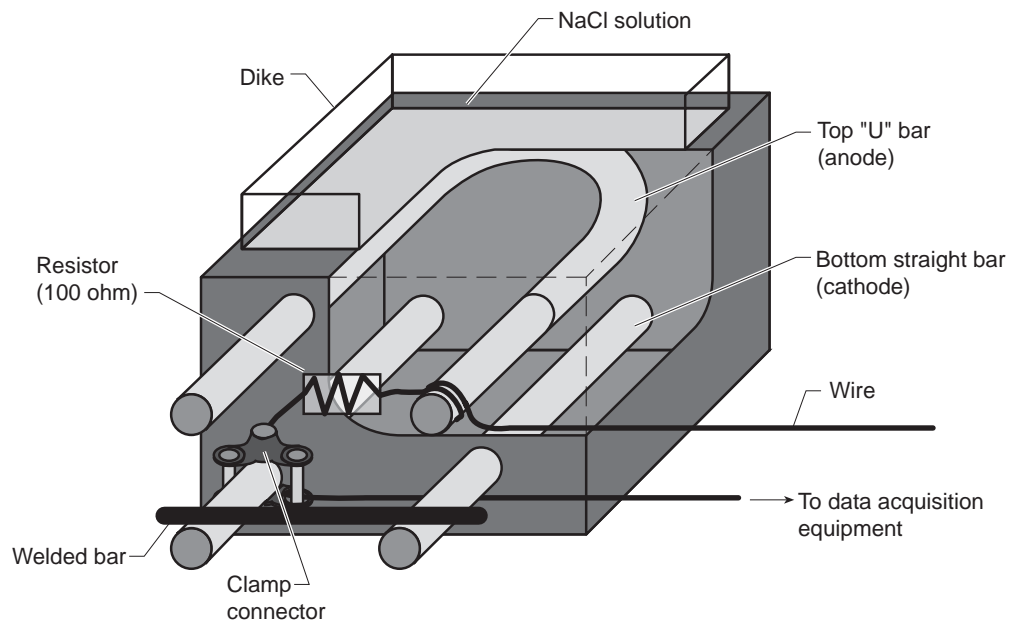


Figure 2.11: Typical Project 1265 Macrocell Specimen

The only difference between the #4 bar and #6 bar macrocells was a slight modification of the bar placement. These modifications were made to accommodate the larger diameter of the

#6 bar so that the depth of concrete cover was 1 inch and the clear spacing between the top layer and bottom layer of steel was 4 inches for both sets of macrocells.

2.4 CONSTRUCTION OF MACROCELL SPECIMENS

2.4.1 Bar Preparation

All of the bars received, except for the galvanized A and nonbendable epoxy-coated bars, were not the required length and were straight. The cutting and bending of the bars was performed offsite at an epoxy-coating bar manufacturing facility. The bars were first sheared to the required length. Then several of the bars were bent into a “U” shape for the top layer of steel. Plastic mandrels were used in the bending process to minimize any damage to the coatings.

The shearing process exposed the cross section of the bars, which was left unprotected and was susceptible to corrosion during testing. Care was taken to exclude as many of the sheared bar ends from being embedded within the macrocell; however, this was not entirely possible. Epoxy was used to patch any of the sheared ends that were embedded within the macrocells.

It was observed that the shearing of the 304 stainless steel-clad bars caused the cladding to separate from the underlying mild steel core (see Figure 2.12). The separation of the cladding from the core probably would compromise the corrosion protection of the bar and affect the monitoring results of the macrocell testing. The separations were removed with a grinding wheel, and the exposed core and stainless steel cladding at the end were patched with epoxy.

Both sets of galvanized bars and the nonbendable, epoxy-coated bars were received already bent. The nonbendable, epoxy-coated bars were bent prior to the coating process because this epoxy is brittle and will crack when bent. The galvanized A bars were bent after the galvanizing process, and the galvanized B bars were bent prior to being galvanized. The results of the galvanized bars will be compared to determine if the bending process might have an effect on the corrosion resistance.

The galvanized A and nonbendable epoxy bars have a smaller inside diameter than the minimum required diameter of six times the diameter of the bar. This should not influence the

corrosion behavior of the nonbendable, epoxy-coated material because the bars were bent prior to the coating process; however, it may influence the behavior of the galvanized A bars.



Figure 2.12: Separation of Stainless Steel Cladding from Shearing

2.4.2 Formwork and Bar Placement

The formwork was designed to hold sixteen macrocell specimens, and all of the macrocells for a particular test material could be cast in one set of formwork. Eleven sets of forms were constructed so that all 176 macrocells could be cast simultaneously. Screws were used to assemble the pieces of the formwork. The two rows of macrocells within the forms were slightly offset for access to fasten the transverse dividers to the longitudinal center divider. Holes were drilled in the two longitudinal perimeter pieces to allow the ends of the “U”-shaped and straight bars to protrude from the concrete prism. The drilled holes were centered within the macrocell and provided the proper concrete cover and bar spacing.

The macrocell bars were only supported by the formwork. The bars were secured by inserting wedges between the formwork and the protruding bars. No chairs or other types of reinforcing bar supports were used within the macrocell. Chairs create discontinuities in the concrete prism, which might affect the penetration of chloride ions into the concrete.

The formwork for the #4 epoxy-coated bars and #6 304 stainless steel-clad bars is typical of the other sets of forms constructed and can be seen in Figures 2.13 and 2.14, respectively.



Figure 2.13: Typical Formwork for Macrocells with #4 Bars



Figure 2.14: Typical Formwork for Macrocells with #6 Bars

2.4.3 Concrete Casting

As stated earlier, eleven sets of forms were constructed to enable simultaneous casting of all 176 macrocell specimens. The macrocells were cast indoors. A local ready-mix company supplied the concrete. Wheelbarrows and shovels were used to place the concrete in the formwork. The concrete was consolidated with a rubber head vibrator, shown in Figure 2.15.

It was observed that the method of securing the bars with wedges worked moderately well. The majority of the bars did not shift during casting. However, there were several instances when the vibrator head struck the bars, and the wedges did not prevent the bars from shifting.

The top surfaces of the macrocells were trowel finished. After the initial set of the concrete, the formwork was covered with wetted curing blankets and plastic sheets to create a moist curing environment and to prevent shrinkage cracks. It is especially important to take proper curing precautions because cracking would likely affect the long-term, corrosion-monitoring results. Curing of the concrete is shown in Figure 2.16.



Figure 2.15: Macrocell Concrete Placement



Figure 2.16: Curing of Macrocell Specimens

The formwork was removed from the specimens over a period of 2 days. There was not enough available room indoors to allow the concrete to finish curing. After the forms were removed, the macrocells were moved outside. Wetted curing blankets covered the macrocells outside for an additional 3 weeks to allow for further curing of the concrete.

After the concrete had sufficiently cured, the top surfaces of the macrocells were sandblasted to remove the layer of cement paste that rises to the surface during troweling. After sandblasting, the macrocells were moved inside.

2.4.4 Saltwater Reservoir

The dams for the saltwater reservoir were constructed from 1/8-inch thick acrylic plates. The acrylic plates were joined end-to-end to form an open box. The plates were chemically welded with a solvent. Once assembled, the dimensions of the dam were 9 inches long by 8 inches wide by 3 inches high. About ¼-inch bead of silicone caulk was applied around the interior and exterior of the base to prevent leakage. The approximate area of the macrocell that is exposed to the saltwater solution is 66 square inches or about 73 percent of the top surface. The acrylic dam can be seen in Figure 2.16.

2.4.5 Electrical Wiring

The protruding ends of the bars were connected so that the electrical potential of the macrocell could be measured. The flow of current in the macrocell is an indication of the level of corrosive activity and can be calculated from the measured voltage. The wiring configuration used in this project is slightly different from the wiring in Figure 2.11 for Project 1265.

In this project, metal clamps were attached to one end of the top bar and to each of the bottom bars. A 100 Ω resistor was soldered between the clamp on the top bar and one of the clamps on the bottom bars. The bottom bars were connected by a copper wire that was soldered at each end to the clamps. The wiring configuration can be seen in Figure 2.17.

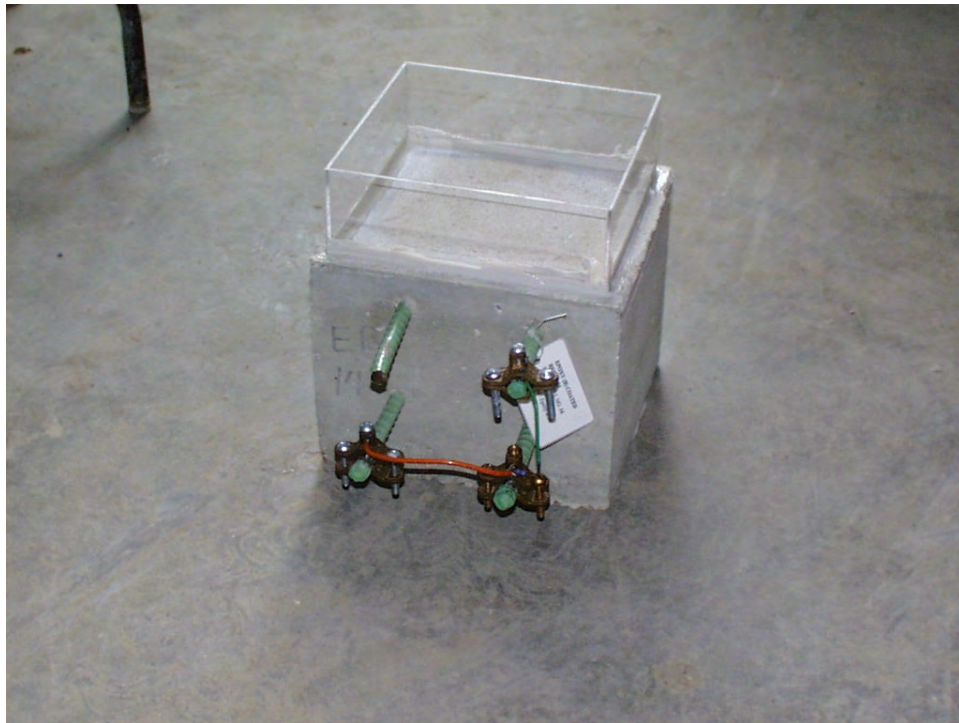


Figure 2.17: Completed Macrocell Specimen

2.4.6 Storage

After the dams and wiring were completed, the macrocells were placed on large storage racks located inside the laboratory building. The room containing the storage racks was

protected from wind and rain, but the room did not have any climate control equipment. The storage racks containing the macrocells can be seen in Figure 2.18.



Figure 2.18: Macrocell Storage Racks

2.5 MATERIAL PROPERTIES

2.5.1 Bar Properties

The American Society for Testing and Materials (ASTM) publishes A615 “Standard Specification for Deformed and Plain Billet-Steel Bars for Concrete Reinforcement” and A775 “Standard Specification for Epoxy-Coated Reinforcing Steel Bars.” A summary of the deformation and coating properties required for #4 and #6 bars by these specifications can be found in Table 2.2.

Table 2.2: ASTM A615 and A775 Requirements

Bar Size	Nominal Diameter (in.)	Deformation Requirements (inches)			Epoxy-Coating Requirements
		Minimum Average Spacing	Minimum Average Height	Maximum Gap	Thickness (0.001 in.)
4	0.5	0.350	0.020	0.191	7-12
6	0.75	0.525	0.038	0.286	7-12

Measurements of the bar deformation and coating properties were taken from a random sampling of bars when received from the manufacturer. The bar deformation properties were recorded using Mitutoyo Digimatic digital calipers, and the coating thickness was measured using a Mikrotest thickness gage (Figure 2.19). The measurements are listed in Table 2.3 and include the average deformation spacing, average deformation height, average gap between deformations, and average coating thickness. The weight of the bar was not measured because an accurate correction for the weight of the coating was not possible.



Figure 2.19: Digital Calipers and Coating Thickness Gage

Table 2.3: Measured Bar Deformation and Coating Properties

Bar Type	Bar Size	Deformation Pattern	Deformation Measurements (in.)			Coating Measurements (0.001 in.)		
			Average Spacing	Average Height	Average Gap	Average Thickness	High	Low
Control A (Black Steel)	4	Parallel & Diagonal	0.310	0.073	0.127	N/A	N/A	N/A
Galvanized A	4	Parallel	0.333	0.047	0.164	7.5	10	6
Galvanized B	4	Diagonal	0.339	0.054	0.186	9.4	13	7
Epoxy A	4	Parallel	0.324	0.059	0.154	13.1	15	11
Epoxy B	4	Parallel	0.313	0.049	0.177	11.7	13	10
Nonbendable Epoxy	4	Diagonal	0.347	0.066	0.167	13.0	17	10
Nylon	4	Diagonal	0.267	0.058	0.122	17.2	21	12
PVC	4	Diagonal	0.309	0.035	0.172	10.2	15	6
304 Stainless Steel	4	Diagonal	0.331	0.062	0.164	N/A	N/A	N/A
Control B (Black Steel)	6	Parallel	0.497	0.079	0.245	N/A	N/A	N/A
Epoxy A	6	Parallel	0.505	0.082	0.259	12.3	14	10
304 Stainless Steel-Clad	6	Diagonal	0.462	0.109	0.147	33.7	39	28

2.5.2 Concrete Properties

As stated above, the concrete for the macrocells was ordered from a local ready-mix company. A four-sack mix without fly ash and with a water-to-cement ratio of about 0.6 was ordered. There were a few unanticipated modifications to the concrete mix by the ready-mix company. Fly ash was added to the mix, and the actual water-to-cement ratio of the concrete was only 0.4. These modifications will increase the durability of the concrete by decreasing its permeability. No water was added onsite. The concrete batch data and tested compressive strength are listed in Table 2.4.

Table 2.4: Concrete Batch Data

Maximum Aggregate	3/4 inch
Cement	423 lb/cy
Water	166 lb/cy
Course Aggregate	1822 lb/cy
Fine Aggregate	1340 lb/cy
Fly Ash	99 lb/cy
Compressive Strength	7170 psi

Casting of the macrocell specimens took place on July 6, 1999. The weather and concrete conditions at the time of casting are listed in Table 2.5.

Table 2.5: Conditions during Macrocell Casting

Air Temperature	81° F
Relative Humidity	57%
Concrete Temperature	91° F
Air Content	8%
Slump	3-4 inches

The concrete compressive strength was tested after 28 days. Cylinders of the concrete were taken before casting, during casting, and after casting. The purpose of taking these cylinders was to determine if there were significant changes in the concrete throughout the casting operation. The tested compressive strengths of the concrete are listed in Table 2.6. The concrete strength was greatest at the beginning of casting with a compressive strength of approximately 8,000 psi. The concrete strength decreased during casting and stabilized around 6,700 psi.

Table 2.6: Macrocell Concrete Compressive Strength

Cylinders	Compressive Strength (psi)
Before Casting	8,030
During Casting	6,620
After Casting	6,860

2.6 EXPERIMENTAL PROGRAM

2.6.1 Chloride Exposure

The long-term exposure to chlorides began after the macrocells were completed and placed on the storage racks. To expose the concrete to chlorides, a saltwater solution with 3.5% NaCl was ponded in the reservoir on the macrocell. The ponding will occur over a 4-week cycle on a 2-week wet/2-week dry basis. The reservoirs are covered with plywood after the saltwater solution is added to limit the amount of evaporation. Pictures of the saltwater preparation and ponding can be seen in Figures 2.20 – 2.22.



Figure 2.20: Researcher Making 3.5% NaCl Solution at the Beginning of the “Wetting Cycle”



Figure 2.21: Researcher Pouring 3.5% NaCl Solution in Dikes at Beginning of “Wetting Cycle”



Figure 2.22: Student Placing Plywood Sheet over Macrocell-Filled Dikes to Minimize Evaporation

A close-up view of macrocells with top bars only and bottom bars only can be seen in Figures 2.23 and 2.24.



Figure 2.23: Macrocells with One Bent Black Rebar as Top-Reinforcing Layer and None in the Bottom-Reinforcing Layer



Figure 2.24: Macrocells with Two Straight Black Rebars as Bottom-Reinforcing Layer and None in the Top-Reinforcing Layer

2.6.2 Corrosion Monitoring

As stated above, current flow can be used to monitor the amount of corrosion in the macrocell. Corrosion readings were taken weekly. The voltage was measured across the 100Ω resistor with the Fluke 8060A True RMS Multimeter shown in Figure 2.25. The current was calculated from the potential using the equation $I = V/R$, where I is the electrical current, V is the measured electrical potential, and R is the resistor rating (100Ω). Also, the condition of the concrete was monitored visually for signs of staining and cracking.

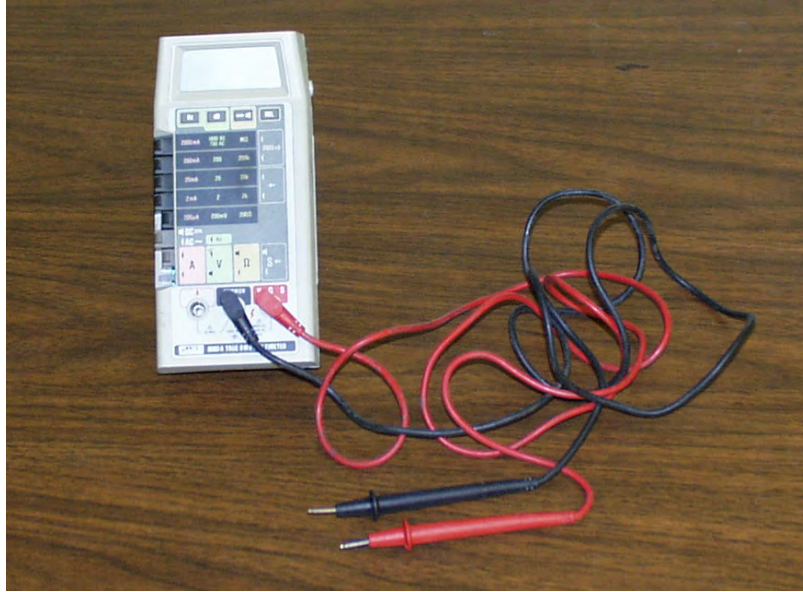


Figure 2.25: Multimeter

The saltwater exposure cycles have been conducted for more than 2 years. To date, there have been only very small changes in the current flow for any of the test materials.

2.6.3 Additional Testing

Monitoring the current flow of the macrocell is only an indirect method of monitoring corrosion. Several additional tests were planned that will give a better understanding of the corrosive activity of the test materials. At least one specimen from each of the candidate materials will be autopsied to observe the condition of the metal. The condition of each bar will be well documented and chemical analysis of the corrosion products will be performed where appropriate. Also, polarization resistance tests will be performed on the macrocells with only the top corrosion resistant bar.

2.7 TEST RESULTS

A sample sheet for test observation and results is shown in Table 2.7.

Table 2.7: Macrocell Ponding Test

Bar Type:

Bar size:

Manufacturer:

Data: Resistance = 100 ohms

Formula: Voltage (V) = Current (I)*Resistance (R)

Wetting Cycle Number: 1

Date of Ponding:

Date of Solution Removal:

Test Performed On:

Macrocell	Voltage	Current
1	0	0
2	0	0
3	0	0
4	0	0
5	0	0
6	0	0
7	0	0
8	0	0
9	-	-
10	-	-
11	-	-
12	-	-
13	0	0
14	0	0
15	0	0
16	0	0

Comments:

- At the time of the initial writing of this report, five wetting-drying cycles were completed.
- Voltage readings were still zero on all of the rebars.
- According to previous studies (Kahhaleh et al. 1994, Kahhaleh et al. 1994), it took almost 6 to 7 months to observe some corrosion values for black steel. Therefore, the onset of corrosion should occur in 6 months or more, because the quality of the concrete is better.

Chapter 3:

Corrosion Evaluation Using Polarization Resistance: Test Principle, Test Results and Discussions

3.1 INTRODUCTION

The polarization resistance (PR) method is useful in both research and engineering applications. It has some advantages over the other methods, as usually only a few minutes are required to determine the corrosion rate. The conventional weight-loss methods require several days or more. PR methods are nondestructive and may be used many times to measure corrosion rates as a function of time on the same electrode.

3.1.1 History and Description

Early researchers (Davison 1987) observed experimentally that the degree of polarization at a given applied current was greater for a lower corrosion rate. An apparent linearity was observed at the origin of the polarization curve for overvoltages up to a few millivolts. Thus, the slope of this linear curve is inversely proportional to the corrosion rate. The method is sometimes referred to as the linear polarization method.

PR, defined as the slope of the polarization curve at the origin, is independent of the degree of linearity.

$$R_p = [d\epsilon / di_{app}]_{\epsilon \rightarrow 0} = \Delta\epsilon / \Delta i_{app} = B / i_{corr}$$

Therefore, the slope, $([d\epsilon / di_{app}]_{\epsilon \rightarrow 0})$, at the origin of the polarization curve, defined as polarization resistance, is inversely proportional to the corrosion rate, where

$$B = \beta_a \beta_c / 2.3 (\beta_a + \beta_c)$$

is the proportionality constant. The Tafel constants, β_a , the anodic Tafel constant and β_c , the cathodic Tafel constant, can be determined experimentally.

3.1.2 Test Set-Up

Normally, the working electrode (specimen to be tested) is a small button prepared, cleaned, and polished just 1 hour prior to experimentation. The entire PR test assembly is designed, keeping in mind the small button specimen (ASTM G5-94 (Reapproved 1999), *Standard Reference Test Method for Making Potentiostatic and Potentiodynamic Anodic Polarization Measurements*) (ASTM G5-94, 1999).

However, in this project, the specimens or the working electrodes were bent #4 or #6 bars; hence, considerable changes had to be made to the test cell to fit the large working electrode. See Figure 3.1 for details.

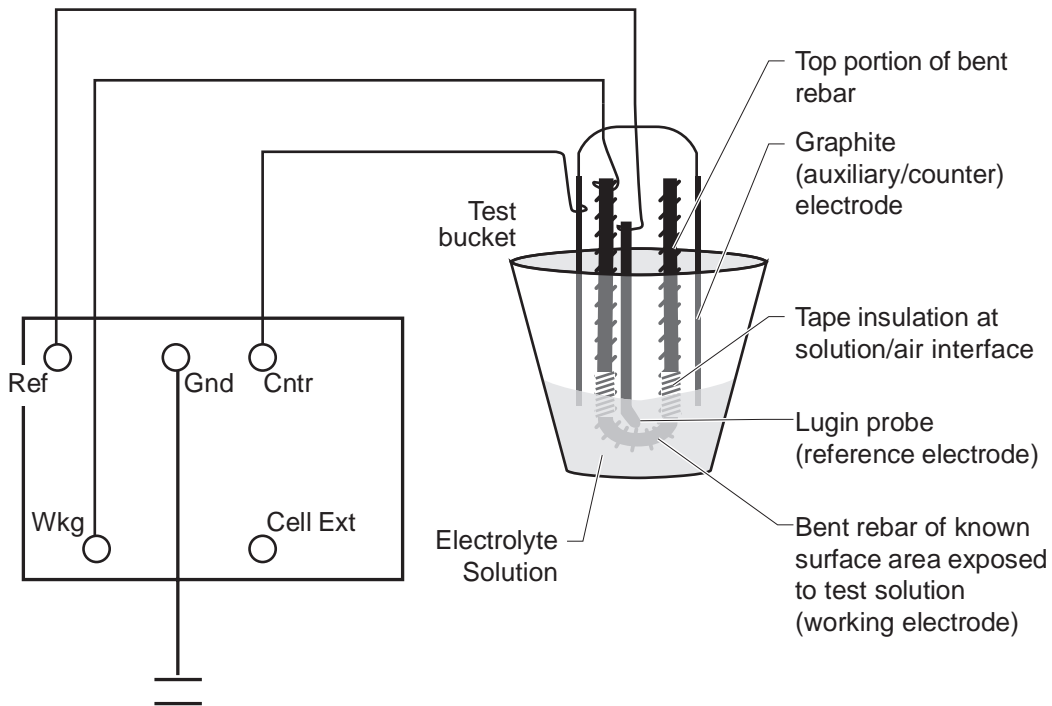


Figure 3.1: Schematic Diagram of Polarization Resistance Test Cell

3.1.3 Electrolyte / Solution

The PR tests were conducted for a period of 6 days. Electrolytes were used for 2 days each. For the first 2 days, saturated calcium hydroxide solution was used (1.85 g Ca(OH)₂/liter of water). For the third and fourth days, an additional threshold amount of NaCl was added (0.67 g NaCl/liter of water). For the fifth and sixth days, more NaCl was added for a total amount of NaCl present in the test cell of 3.5% (about 35 g NaCl/liter of water). Calcium hydroxide was used as an electrolyte as it simulates the alkaline pore solution of concrete. A stable passivation layer may be formed after 2 days of exposure to this electrolyte (Elsener 1991). Sodium chloride solution was used to simulate the conditions of the real-life concrete structures exposed to deicing salts.

3.2 TEST PROCEDURE

- A particular rebar specimen was selected to be the working electrode.
- The tip of the working electrode was ground off, if it was a coated rebar, to facilitate proper electrical connections.
- The tip was polished as shown in Figure 3.2.
- The working area (the portion of the rebar to be exposed to the electrolyte) of the rebar was cleaned and degreased.
- The surface area of the rebar portion to be exposed was measured (in square cm).

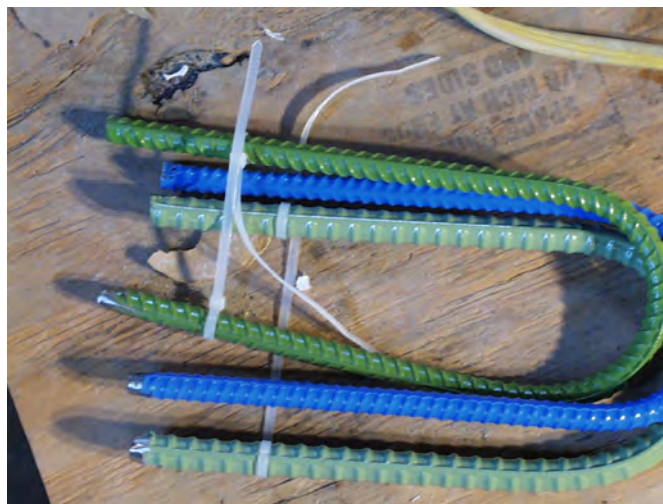


Figure 3.2: Polymer-Coated Rebars with Their Tips Polished to Ensure Good Electrical Contact during Polarization Resistance Test



Figure 3.3: Polarization Resistance Test Cells without Connections

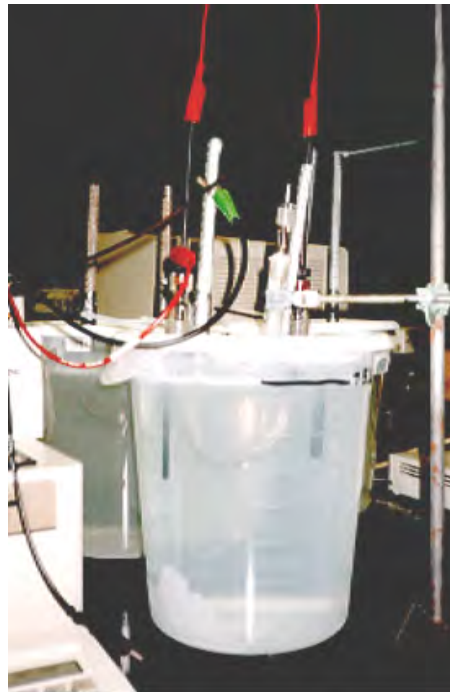


Figure 3.4: Polarization Resistance Test Cells with Connections

The density and equivalent weight of the rebar materials were determined from standard tables as shown in Table 3.1.

Table 3.1: Density and Equivalent Weight of Various Materials

Metal / Alloy	Density (g/cc)	Equivalent Weight
Iron/Steel	7.87	27.92
Zinc	7.13	32.69
SS304	7.9	25.112

Source: Adapted from Proposed Standard, ASTM G01.11, ASTM, Philadelphia

For galvanized rebars, the constants for zinc were used. The PR test has limited use for coated bars unless there are pinholes in the coatings. These coatings were essentially defect free and thus the coated bars were not tested using this method.

- The level of the solution was to cover the bend and adjacent areas, and the remaining portion of the rebar was insulated with tape to avoid its contact with the electrolyte. Also, epoxy adhesive was placed on the tape to minimize crevice corrosion.
- Holes of appropriate diameter were drilled in the lid of the test cell as shown in Figure 3.5.



Figure 3.5: Lid of Polarization Resistance Test Cell with Holes to Accommodate the Rebar, the Reference Electrode and the Lugin Probe

- Graphite electrodes and the reference electrode were inserted into the test cell along with the working electrode.
- The rebar depth was adjusted so that the lugin probe/reference electrode assembly was perpendicular to the bent portion of the rebar.
- The cell was filled with the appropriate electrolyte.
- Connections were made as shown Figure 3.1.
- All cell connections were ensured.
- The toggle clamp of the cell was switched from DUMMY to EXT.
- The cell button on the potentiostat was pressed to ON position.
- Initial test data were recorded on the computer.
- The test was started. A sample test sheet is shown in Table 3.2.

Table 3.2: PR Sample Test Sheet (for Black Steel)

Test: Polarization Resistance	Test Code: PR BLK
Test Date:	Electrolyte: Sat. Ca(OH) ₂ with or without chloride contamination
Area: 89.3 sq.cm	Equivalent Weight: 27.92
Density: 7.87 g/cc	Cathodic Tafel Constant: PASS
Anodic Tafel Constant: PASS	Delay: 200 sec
Sample Results:	
E(corr)= -0.1250 V	
Corr. Rate = 0.1896 mpy	
Polarization Resistance = 47.34 k-ohm-cm ²	

Note: Six readings were taken for each sample. Though six readings were taken in 6 days, they were taken at different times. Reading 1 was taken within 2 hours after introducing the rebars in the calcium hydroxide. Reading 2 was taken at the end of the 2-day exposure period, i.e., just before adding the threshold amount of NaCl. Reading 3 was taken soon after adding the threshold amount of NaCl. Reading 4 was taken at the end of this period, i.e., just before adding NaCl to reach 3.5% NaCl. Reading 5 was taken soon after adding 3.5% NaCl and reading 6 was taken at the end of this 2-day period.

3.3 TEST RESULTS:

While all of the types of bars were immersed in the solutions as discussed in the previous section, PR tests were carried out for black steel, stainless steel 304 rebar, galvanized A rebar, and galvanized B rebar. The results are discussed below and shown in Tables 3.3 through 3.11 and Figures 3.6 through 3.14.

3.3.1 Black Rebar

Table 3.3: Corrosion Rate and PR versus Salt Concentration for Black Steel

Salt Concentration (mol/L)	Corrosion Rate (mpy)	Polarization Resistance (k-ohm cm ²)
0	0.1896	47.34
0.01146	1.79	4.56
0.51334	3.15	3.182

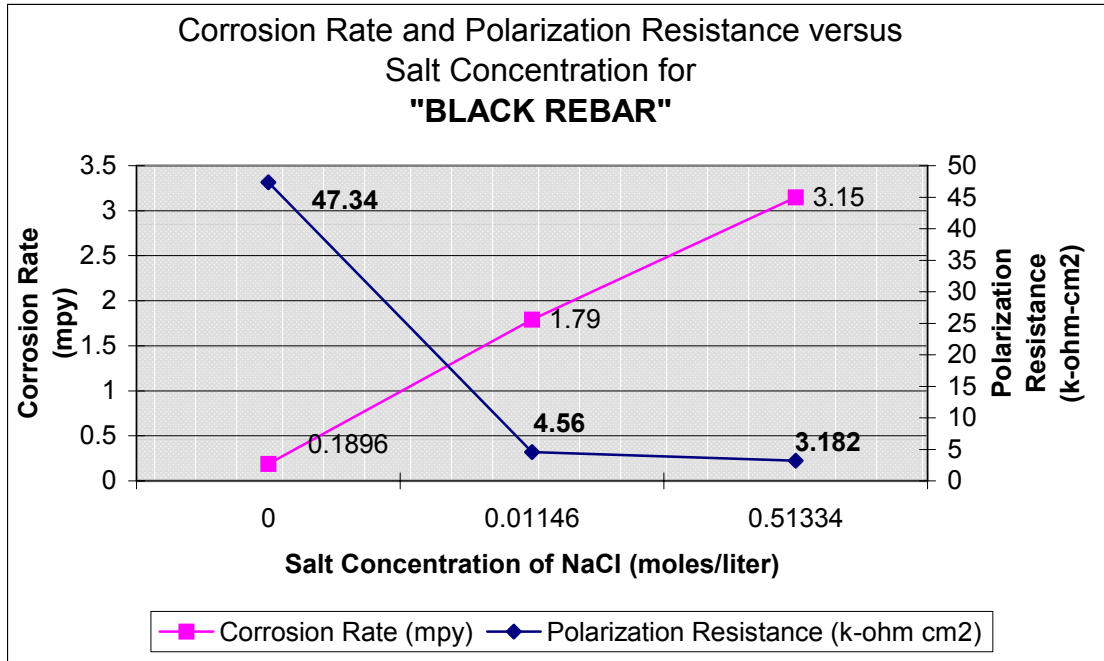


Figure 3.6: Corr. Rate and PR versus Salt Concentration for Black Steel

The corrosion rate increased steadily with increasing chloride concentration (as shown in Table 3.3 and Figure 3.6). The corrosion rate of black steel in calcium hydroxide solution contaminated with 3.5% NaCl was 1.75 times the corrosion rate in calcium hydroxide contaminated with the threshold amount of NaCl (Figure 3.6).

The PR of the black steel decreased with increasing chloride concentration. The corrosion rate, which is inversely related to the polarization resistance, versus the day of exposure is shown in Table 3.4 and Figure 3.7 for the black steel.

Table 3.4: Corrosion Rate versus No. of Days for Black Steel

Day	Corrosion Rate (mpy)
1	0.8686
2	0.1896
3	1.56
4	1.79
5	2.6
6	3.15

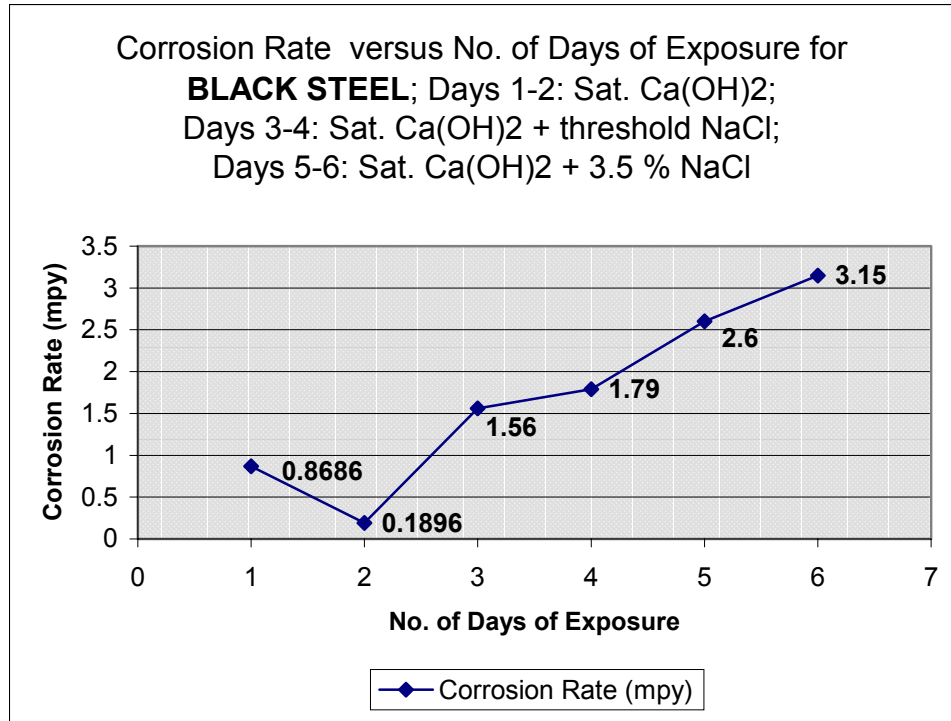


Figure 3.7: Corr. Rate versus No. of Days for Black Steel

There was an initial drop in the corrosion rate during the 2-day exposure to calcium hydroxide solution (Figure 3.7), which may be due to the formation of a passivation layer. However, the corrosion rate once again increased on addition of increasing amounts of NaCl, indicating possible damage to the protective passivation layer.

3.3.2 Pure Stainless Steel 304 Rebar

The corrosion information for the 304 stainless steel rebar is shown in Tables 3.5 and 3.6 and Figures 3.8 and 3.9.

Table 3.5: Corrosion Rate and PR versus Salt Concentration for SS304

Salt Concentration (mol/L)	Corrosion Rate (mpy)	Polarization Resistance (k-ohm cm ²)
0	0.0259	346.68
0.01146	0.0153	584.91
0.51334	0.2499	51.77

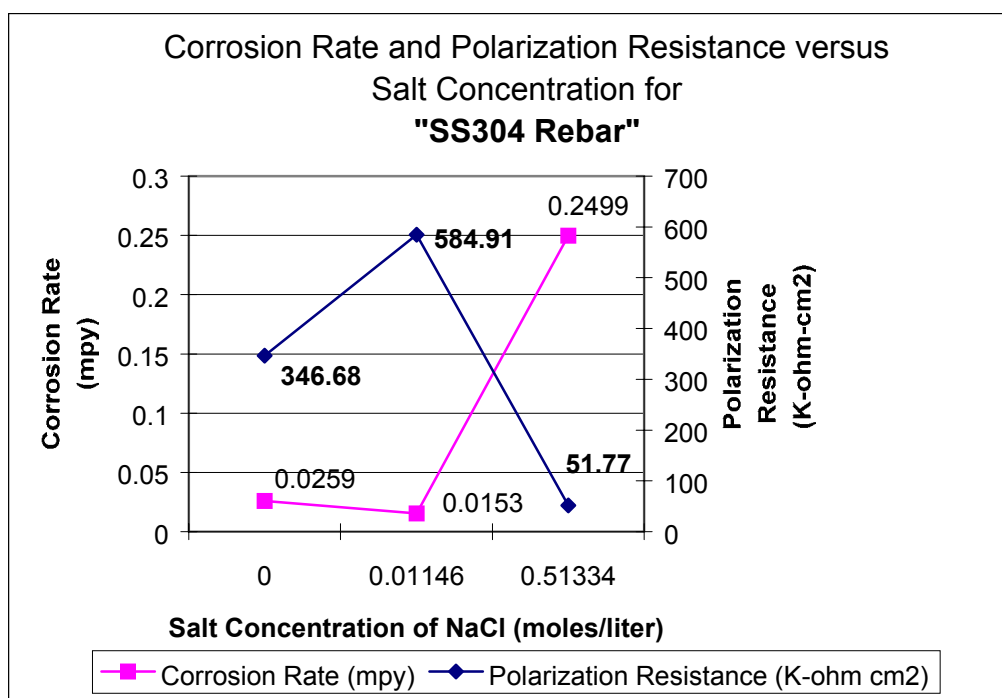


Figure 3.8: Corr. Rate and PR versus Salt Concentration for SS304 Rebar

As expected, the pure stainless steel 304 rebar performed exceedingly well compared to the black steel. There was a twelve-fold decrease in PR value on increasing the chloride concentration from the threshold amount to 3.5%. Therefore, the corrosion rate value increased drastically with the increase in chloride concentration from the threshold amount to 3.5% NaCl. This showed significant dependence of the corrosion rate of SS304 on the concentration of chloride ions. However, the maximum corrosion rate was still low (0.2499 mpy) when compared to black steel.

Table 3.6: Corrosion Rate versus No. of Days for SS304

Day	Corrosion Rate (mpy)
1	0.3854
2	0.0259
3	0.0242
4	0.0153
5	0.1556
6	0.2499

There was an initial drop in the corrosion rate after 1 day of exposure to calcium hydroxide solution, again indicating possible formation of a passive oxide layer (Figure 3.9). This layer was perhaps damaged on addition of chloride concentration greater than the threshold amount.

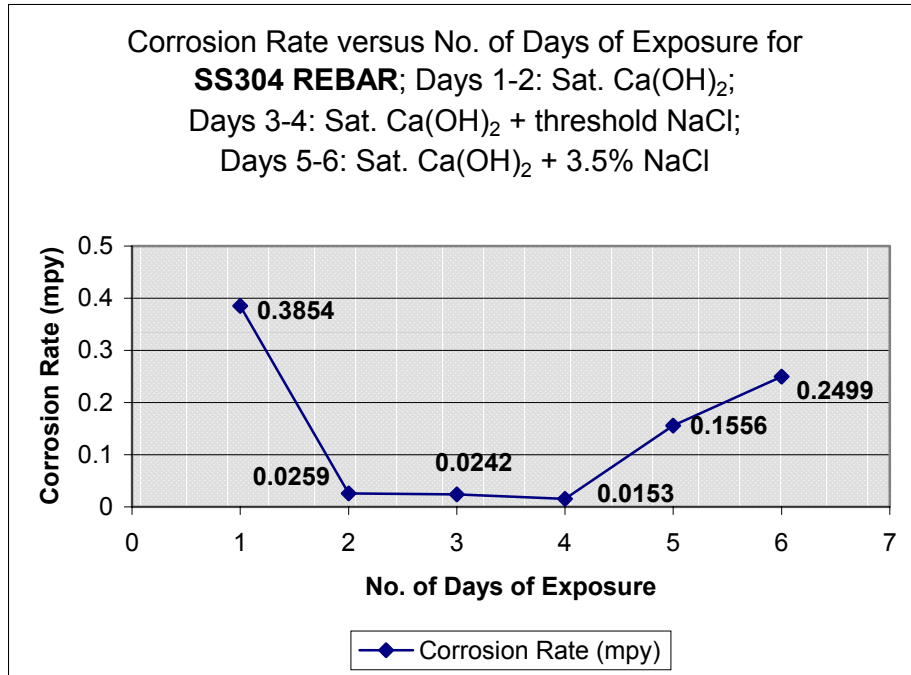


Figure 3.9: Corr. Rate versus No. of Days for SS304 Rebar

3.3.3 Galvanized A Rebar

The corrosion information for the galvanized A rebar is shown in Tables 3.7 and 3.8 and Figures 3.10 and 3.11.

Table 3.7: Corrosion Rate and PR versus Salt Concentration for Galv. A Rebar

Salt Concentration (mol/L)	Corrosion Rate (mpy)	Polarization Resistance (k-ohm cm ²)
0	0.6979	18.54
0.01146	0.1311	98.74
0.51334	1.3	9.98

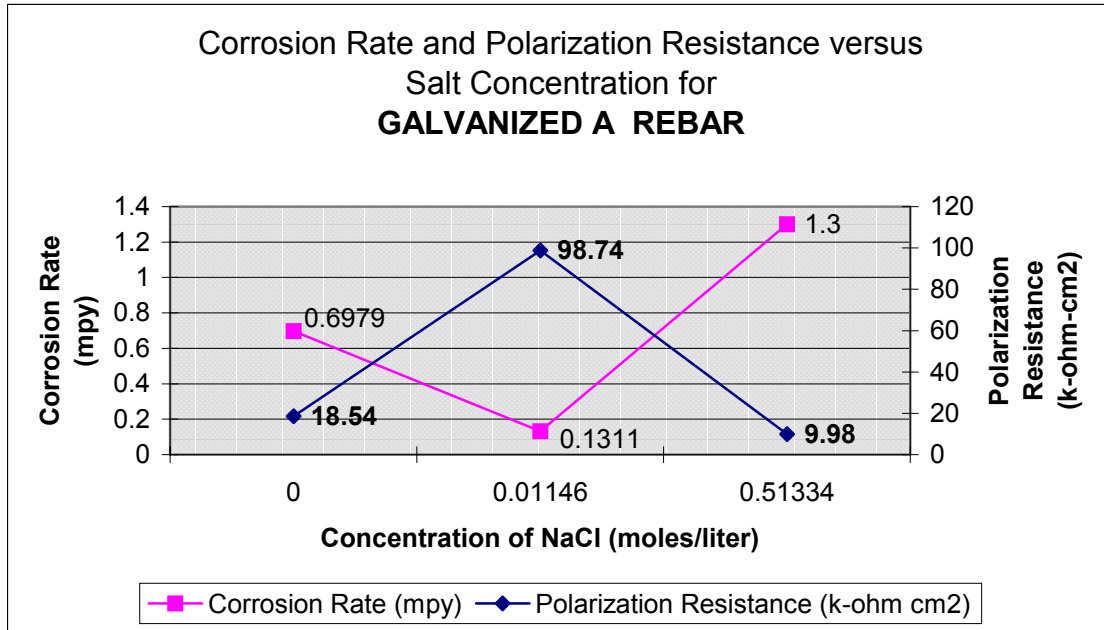


Figure 3.10: Corr. Rate and PR versus Salt Concentration for Galvanized A Rebar

Table 3.8: Corrosion Rate versus No. of Days for Galv. A Rebar

Day	Corrosion Rate (mpy)
1	3.21
2	0.6979
3	0.138
4	0.1311
5	2.72
6	1.3

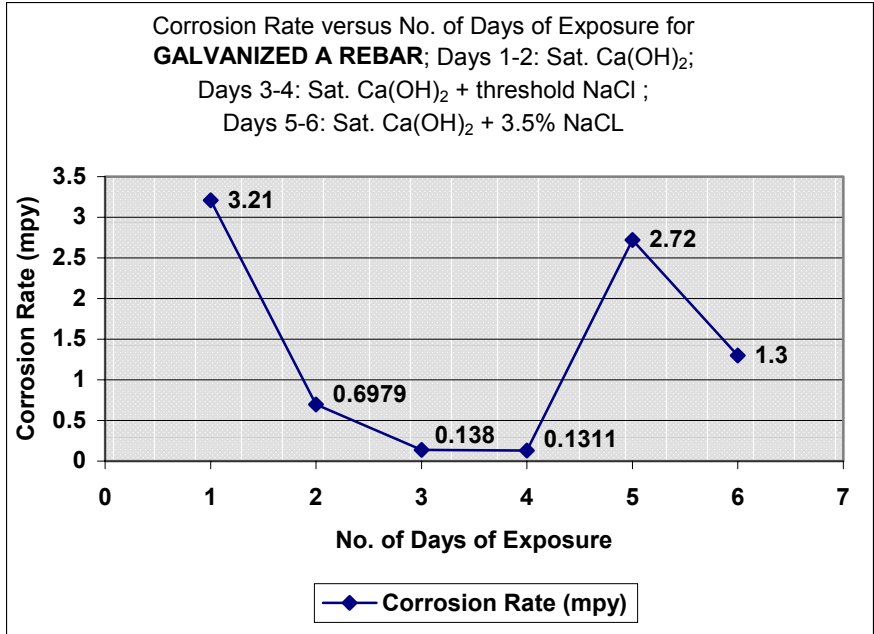


Figure 3.11: Corr. Rate versus No. of Days for Galvanized A Rebar

It is evident that the corrosion rate dropped initially from 0.69 to 0.13 mpy on addition of the threshold amount of NaCl (Figure 3.10). However, it stabilized at a rate of 1.3 mpy after addition of 3.5% NaCl to the calcium hydroxide solution.

3.3.4 Galvanized B Rebar

The corrosion information for the galvanized B rebar is shown in Tables 3.9 and 3.10, and Figures 3.12 and 3.13.

Table 3.9: Corrosion Rate and PR versus Salt Concentration for Galv. B Rebar

Salt Concentration (mol/L)	Corrosion Rate (mpy)	Polarization Resistance (k-ohm cm ²)
0	1.15	11.24
0.01146	0.4679	27.64
0.51334	0.652	19.83

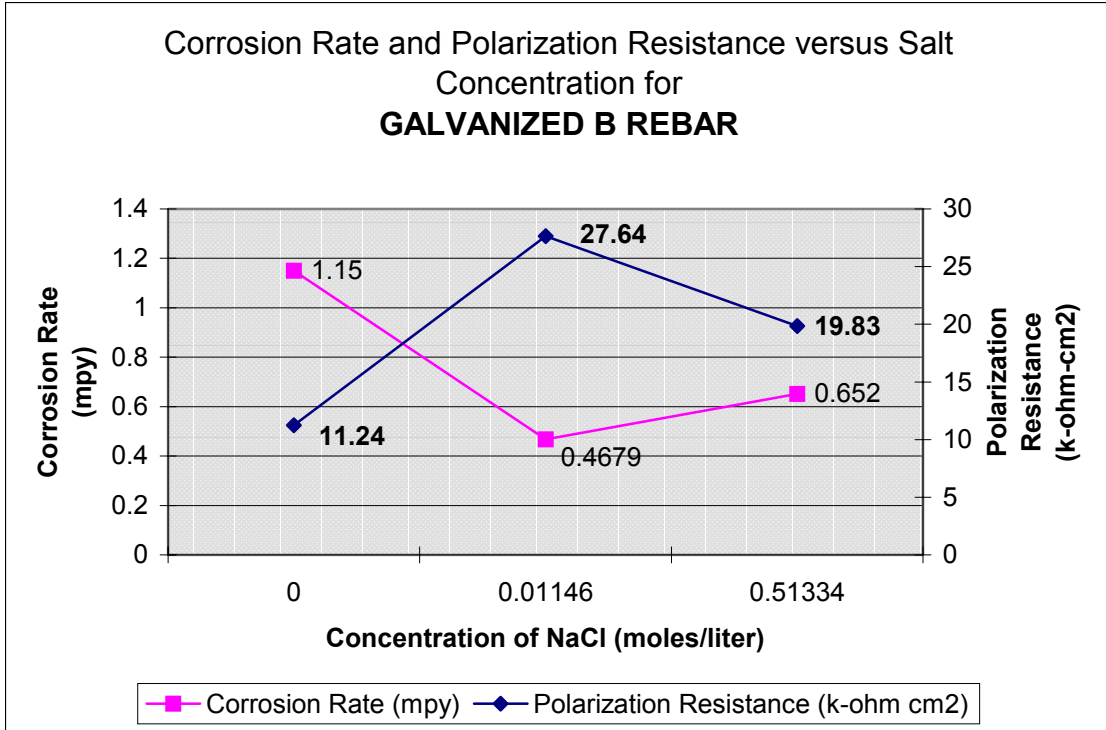


Figure 3.12: Corr. Rate and PR versus Salt Concentration for Galvanized B Rebar

Table 3.10: Corrosion Rate versus No. of Days for Galv. B Rebar

Day	Corrosion Rate (mpy)
1	0.7558
2	1.15
3	3.04
4	0.4679
5	0.6125
6	0.652

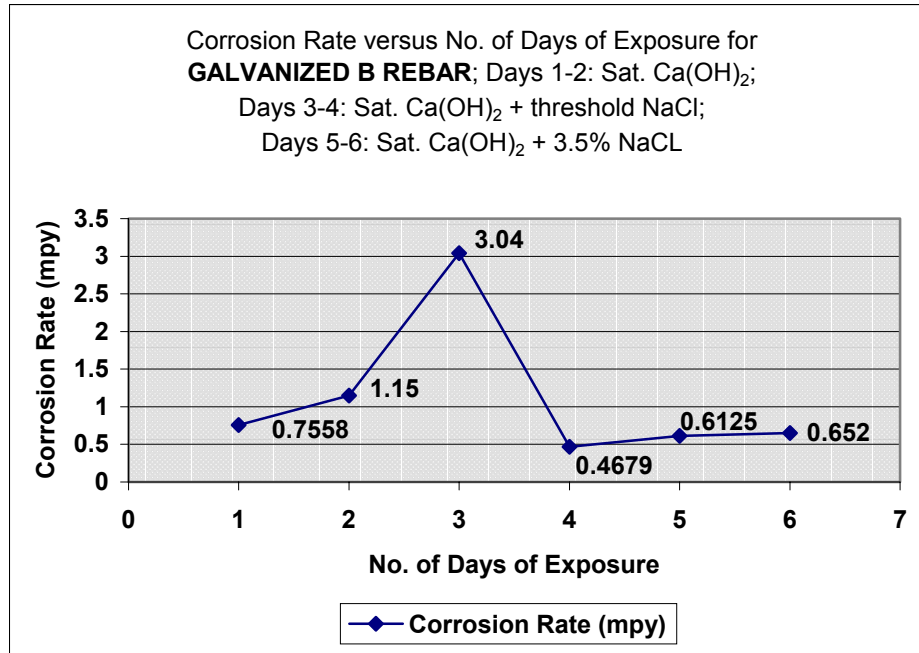


Figure 3.13: Corr. Rate versus No. of Days for Galvanized B Rebar

Once again, it is evident that the corrosion rate dropped initially from 1.15 to 0.46 mpy on addition of the threshold amount of NaCl (Figure 3.12). However, it increased to 0.652 mpy on addition of 3.5% NaCl to calcium hydroxide solution.

3.3.5 Comparison of All Systems

A comparison of the black steel, stainless steel, and galvanized steel is given in Table 3.11 and Figure 3.14.

Table 3.11: Corrosion Rate versus Salt Concentration (of All Systems)

Salt Concentration (mol/L)	Black Steel	SS304 Rebar	Galvanized A	Galvanized B
0	0.1896	0.0259	0.6979	1.15
0.01146	1.79	0.0153	0.1311	0.4679
0.51334	3.15	0.2499	1.3	0.652

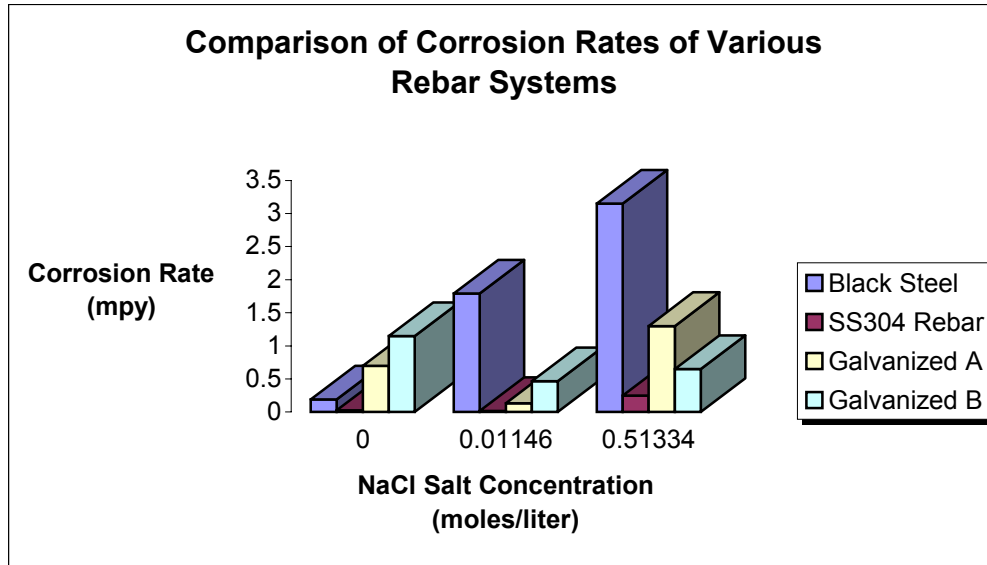


Figure 3.14: Comparison of Corrosion Rates of Various Rebars

It is evident that SS304 rebar performed quite well (Figure 3.14) in all three solutions. It had extremely low corrosion rates and should be an excellent material in the form of a pure rebar or a clad bar (which would be more economical). Black steel, as expected, had the highest corrosion rate in the presence of salt. However, its corrosion rate was less than the corrosion rate of both galvanized A and galvanized B rebars in pure calcium hydroxide solution. Its corrosion rate increased in the presence of salt. Galvanized A rebar performed better than galvanized B rebar in pure calcium hydroxide solution as well as in $\text{Ca}(\text{OH})_2$ plus the threshold amount NaCl. However, in the presence of 3.5% NaCl, galvanized B performed better. The reason may be due to the fact that galvanized B was coated after it was bent, while galvanized A was bent after it was coated. Secondly, galvanized A rebar was bent by the supplier with a bent diameter more stringent than the other rebars included in this project (Figures 2.7 and 2.8). This means that there is a greater chance of damage to galvanized A rebar.

Chapter 4:

Summary and Conclusions

4.1 SUMMARY OF EXPERIMENTAL RESULTS

In this project, three types of tests have been carried out to determine the corrosion evaluation of various reinforcement systems. These include macrocell tests, polarization resistance (PR) and screening tests, and pull-out tests (in Report 4904-3). Section 4.1.1 deals with the macrocell testing, while Section 4.1.2 addresses PR and screening tests.

4.1.1 Summary of Macrocell Tests

At the time of the initial writing of this report, five wetting-drying cycles had been completed on the macrocell tests, and the following conclusions were drawn:

- Voltage readings were still zero on all of the rebars.
- Periodically raising the temperatures of the macrocells may be a possible recommendation, as it would accelerate the tests.

4.1.2 Summary of Polarization Resistance and Screening Tests

Screening tests were carried out for all types of rebars in calcium hydroxide solution with or without varying amounts of sodium chloride. The rebars were exposed to a repeated cycle of 2 days each of pure calcium hydroxide, calcium hydroxide with the threshold amount of NaCl, and calcium hydroxide with 3.5% NaCl. These tests give valuable qualitative information on the nature of corrosion on reinforcements. Three cycles were completed at the time of writing this report. The following conclusions have been drawn:

- Black steel showed considerable corrosion product formation at the solution-rebar interface. However, no other rebar showed corrosion product formation. As demonstrated SS304 rebar performs excellently (Figure 3.14) in all three solutions. It has extremely low corrosion rates and should be an excellent material in the form of a pure rebar or the more economical clad rebar.

- Black steel, as expected, had the highest corrosion rate in the presence of salt. However, its corrosion rate was less than the corrosion rate of both galvanized A and galvanized B rebars in pure calcium hydroxide solution. Its corrosion rate drastically increased in the presence of salt.
- Galvanized A rebar performed better than galvanized B rebar in pure calcium hydroxide solution as well as in $\text{Ca}(\text{OH})_2$ + the threshold amount NaCl. However, in the presence of 3.5% NaCl, galvanized B performed better. The reason may have been due to the fact that galvanized B was coated after it was bent, while galvanized A was bent after it was coated. Secondly, galvanized A rebar was bent by the supplier with a bent diameter more stringent than the other rebars included in this project, which resulted in greater chance of damage to the coating of galvanized A rebar.

The results of the macrocell tests will give real-time analysis of the different rebar samples tested in this project. They could then be coupled with the results of PR tests to arrive at complete conclusions.

BIBLIOGRAPHY

- ASTM G5-94** (Reapproved 1999). “*Standard Reference Test Method for Making Potentiostatic and Potentiodynamic Anodic Polarization Measurements,*” Annual Book of Standards, ASTM, West Conshohocken, PA.
- ASTM G109** (1999). “*Standard Test Method for Determining the Effects of Chemical Admixtures on the Corrosion of Embedded Steel Reinforcement in Concrete Exposed to Chloride Environments,*” Annual Book of ASTM Standards, ASTM, West Conshohocken, PA.
- B. Elsener; M. Buchler; F. Stalder; and H. Bohni.** Migrating Corrosion Inhibitor Blend for Reinforced Concrete: Part 1—Prevention of Corrosion, *The Journal of Corrosion Science and Engineering*, Vol. 55, No. 12, pp 1155 – 1163, 1991.
- Fontana, M. G.** “Corrosion Engineering,” 3rd ed. McGraw-Hill, New York, NY, 1986.
- Gowripalan, N.** “*Chloride-Ion Induced Corrosion of Galvanized and Black Steel Reinforcement in High-Performance Concrete,*” Source: Cement and Concrete Research v 28 n 8 Aug 1998 Elsevier Sci Ltd p 1119-1131.
- Kahhaleh, Khaled; Jirsa, James; Carrasquillo, Ramon; Wheat, Harovel.** “*Macrocell Corrosion Testing of bent Epoxy-Coated Bars in Chloride Solution,*” Proceedings of the Materials Engineering Conference Infrastructure: New Materials and Methods of Repair Proceedings of the 3rd Materials Engineering Conference Nov 13-16 1994 n804 San Diego, CA, USA, p 8-15.
- Kahhaleh, Khaled; Jirsa, James; Carrasquillo, Ramon; Wheat, Harovel.** “*Macrocell Corrosion Study of Fabricated Epoxy-Coated Reinforcement,*” Corrosion and Corrosion Protection of Steel in Concrete, Proceedings of International Conference held at The University of Sheffield, 24-28 July, 1994, Sheffield Academic, R.N. Swamy, Ed., Press, pp 1244 – 1253.
- Lee, S. K. and Hartt, W. H.** “Autopsy Results of Epoxy Coated Steels Embedded in Test Slabs,” Paper no. 634, Corrosion 98, pp 1-3.
- McDonald, D. B.; Sherman, M. R.; Pfeifer, D. W.; Virmani, Y. P.** “*Stainless Steel Reinforcing as Corrosion Protection,*” Concrete International v17 n5 May 1995 American Concrete Inst Detroit Mi USA p 65-70.
- R. M. Davison; T. Debold; and M. J. Johnson.** Metals Handbook, Vol. 13, *Corrosion*, 9th ed., ASM International, Metals Park, Oh, p. 547, 1987.

